Transition Metal Complexes with 'End-off' Compartmental Schiff Bases Containing Sulphonic or Phosphonic Groups

P. GUERRIERO, D. AJO', P. A. VIGATO, U. CASELLATO

Istituto di Chimica e Tecnologia dei Radioelementi del C.N.R., Area della Ricerca, Corso Stati Uniti 4, Padua, Italy

P. ZANELLO

Dipartimento di Chimica dell'Universita', Pian dei Mantellini 44, Siena, Italy

and R. GRAZIANI

Dipartimento di Chimica Inorganica, Metallorganica e Analitica dell' Universita', via Loredan 4, Padua, Italy

Abstract

Nickel(II), manganese(II) and copper(II) complexes with 'end-off' compartmental ligands derived from 2,6-diformyl-4-chlorophenol and α or β-aminosulphonic or aminophosphonic acids, have been prepared.

The mono- and homobinuclear complexes, obtained by template or step by step procedures, have been characterized by IR, UV, scanning electron microprobe analysis and magnetic susceptibility measurements. The electrochemical behaviour of some complexes has been also examined.

The crystal structure of $\{[Cu_2(C_{10}H_8ClN_2O_7S_2)-(OH)](DMSO)(H_2O)\}_2$ has been determined by X-ray crystallography. The compound is orthorhombic, space group *Pbca*, with $a = 17.071(5)$, $b = 11.751(5)$, $c = 20.464(4)$ Å, $Z = 4$. The molecule of the compound is centrosymmetric. One five-coordinate square pyramidal and one four-coordinate square planar copper atom are present in the asymmetric unit, and the four coordinate copper also makes a contact of 2.58 Å with a DMSO molecule.

Selected bond distances are: Cu–O (bridging) 1.95 Å (mean), Cu–O (base) 2.00 Å, Cu–N (base) 1.96 Å (mean), Cu–O (axial) 2.25 Å. The organic ligand is pentadentate; the hydroxo oxygen atom is bridging two copper atoms of the same asymmetric unit and is axially bonded to one copper atom of the centrosymmetric unit. The clathrate water molecules are hydrogen bonded to the compound.

Introduction

Compartmental ligands [1–3], mostly Schiff bases derived from 2,6-disubstituted phenols, 1,3,5-triketones and β-ketophenols, can incorporate two metal ions. Consequently they have value in studying the magnetic interactions between the metal ions, in the preparation of potential homogeneous catalysts capable of carrying out multi-step or different successive processes. Both of these aspects have relevance in the application of homo- and heterobimetallic complexes as models for certain metallobiomolecules [4].

There are three types of these ligands: the macrocyclic form **I**, derived from a '2 + 2' condensation reaction, an 'end-off' acyclic form **II** in which one donor bridge is removed, and a 'side-off' acyclic form **III**, in which one non-donor bridge is removed.
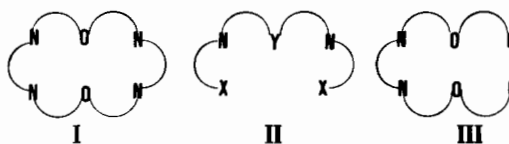

X = O, S, N
Y = O, S

The end-off ligands provide only one endogenous bridging donor atom whereas a further exogenous bridge between the metal sites may be provided by an anion.

These ligands have been obtained by condensation of diformyl- or diacetyl-phenols with a wide range of amines such as dialkylalkanediamines, aminoacids, 2-aminoalkylpyridine, histamine, aminophenols or aminothiophenols, and many metal complexes have been prepared and their physico-chemical properties studied in detail [4].

Comparatively little attention has been devoted to systems derived from 2,6-diformyl-4-chlorophenol and α- or β-aminosulphonic or the analogous phosphonic acids, which can give rise, in principle, to complexes comparable with those obtained by α- and β-aminoacids. A recent paper [5], however, reported a non-compartmental behaviour of the very similar Schiff base *N,N*-(2-hydroxy-5-methyl-1,3-

IV

V
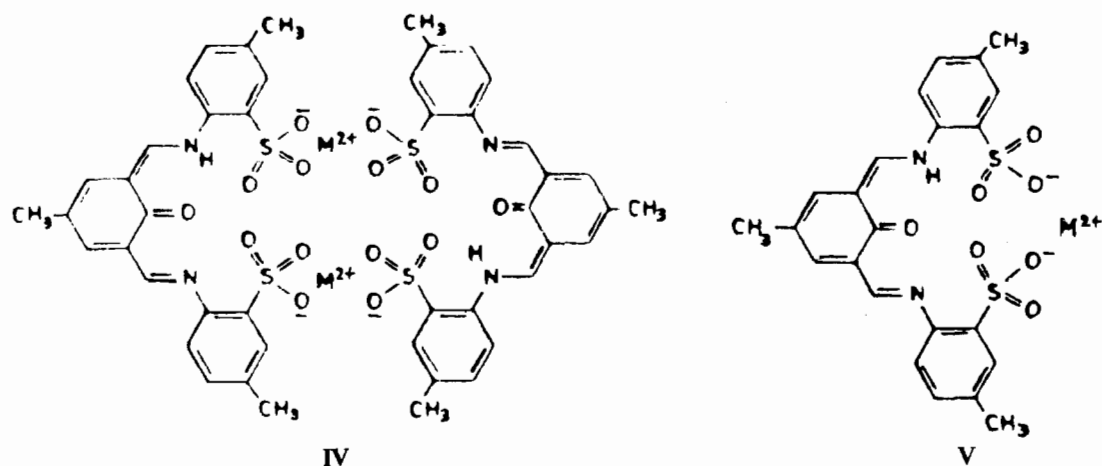
dibenzylidene)-bis-(4-methyl-2-sulphonic acid-aniline). On the basis of electronic and infrared spectra the structures **IV** and **V** were suggested for the two series of prepared complexes.

A similar behaviour was also proposed for the analogous complexes containing naphthosulphonic acids [5].

In order to elucidate the compartmental behaviour of these and similar systems and with the aim of obtaining water-soluble complexes of high paramagnetic ions for their possible use in biological tests we have synthesized and characterized manganese(II), nickel(II) and copper(II) complexes with the Schiff bases H_3L_A, H_3L_B, H_5L_C and H_5L_D:
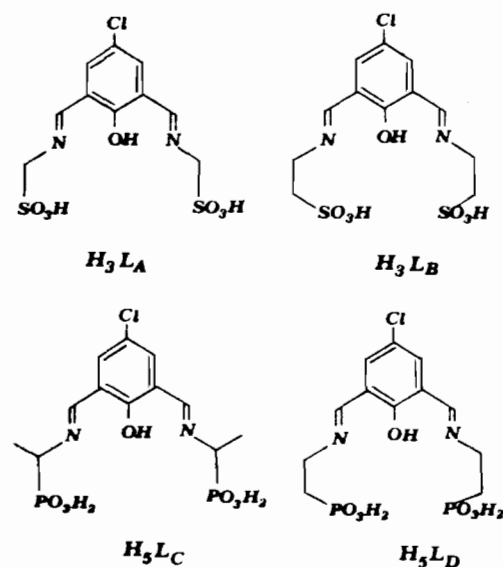
H_3L_A

H_3L_B

H_5L_C

H_5L_D

prepared as trisodium (for sulphonates) and pentasodium (for phosphonates) salts by reaction of 2,6-diformyl-4-chlorophenol with the appropriate amino acids (aminomethanesulphonic acid, 2-aminoethanesulphonic acid, (±)1-aminoethanephosphonic

acid and 2-aminoethanephosphonic acid) in alcoholic solution and in the presence of NaOH. The magnetic and the electrochemical behaviour of the complexes has been studied. Preliminary room temperature susceptibility measurements [6] pointed to significant interactions between Cu(II) ions via phenolic and hydroxyl (or chlorine) bridges. We report here on the variable temperature magnetic susceptibility for the complexes $Cu_2L_ACl \cdot MeOH$, $Cu_2L_AOH \cdot MeOH$, Cu_2L_BOH and $Na_2Cu_2L_DOH \cdot 2H_2O \cdot 2MeOH$.

The crystal structure of the binuclear hydroxo—copper(II) complex with the ligand H_3L_A was also determined by X-ray diffraction.

Experimental

2,6-diformyl-4-chlorophenol was prepared according to the literature [7]; aminomethanesulphonic acid, 2-aminoethanesulphonic acid, (±)1-aminoethanephosphonic acid and 2-aminoethanephosphonic acid were commercial products (Aldrich). Dimethylsulphoxide (Burdick and Jackson) distilled in glass, UV grade, was used as received. Tetraethylammonium perchlorate (Carbo Erba) supporting electrolyte was dried and stored in a vacuum oven at 50 °C. Bis(η^5-cyclopentadienyl)iron(II) (ferrocene) (Alfa-Products) was used as an internal standard. Ultrapure nitrogen was employed to remove oxygen from the tested solutions.

Preparation of Ligand Salts

$Na_3L_A \cdot 3H_2O$ and $Na_3L_B \cdot 2H_2O \cdot MeOH$

To a pale yellow solution of 2,6-diformyl-4-chlorophenol (1.84 g, 10 mmol) in methanol (250 ml), aminomethanesulphonic acid (2.22 g, 20 mmol) for Na_3L_A or 2-aminoethanesulphonic acid (2.50 g, 20 mmol) for Na_3L_B was added. NaOH (1.2 g, 30 mmol) was added to the refluxing suspension and, after 1 h, a yellow—orange precipitate was obtained.

The solvent was partially removed and the yellow–orange product was filtered, washed with diethylether and dried *in vacuo*.

$Na_5L_C \cdot 3H_2O \cdot 2MeOH$ and $Na_5L_D \cdot 3H_2O$

To a pale yellow solution of 2,6-diformyl-4-chlorophenol (1.84 g, 10 mmol) in methanol (250 ml), (±)1-aminoethanephosphonic acid (2.51 g, 20 mmol) for Na_5L_C or 2-aminoethanephosphonic acid (2.51 g, 20 mmol) for Na_5L_D, was added. NaOH (2 g, 50 mmol) was added to the refluxing suspension and, after 1 h, a yellow–orange solution was obtained. The solution was reduced in volume and after cooling, the yellow–orange precipitate obtained was filtered, washed with diethylether and dried *in vacuo*.

Preparation of Mononuclear Complexes

$NiL_E \cdot 2H_2O$ and $NiL_F \cdot 2.5H_2O$

To a pale yellow solution of 2,6-diformyl-4-chlorophenol (184 mg, 1 mmol), in methanol (15 ml), aminomethanesulphonic acid (220 mg, 2 mmol) for NiL_E or 2-aminoethanesulphonic acid (250 mg, 2 mmol) for NiL_F in water (20 ml) was added. Ni(OAc)$_2 \cdot 6H_2O$ (496 mg, 2 mmol) in methanol (15 ml) was added to the refluxing solution. The solution turned green and, after 1 h, a bright green precipitate was formed. The solvent was partially removed and the green product was collected by filtration, washed with methanol, diethylether and dried *in vacuo*.

Preparation of Binuclear Complexes

$Cu_2(L_A)OH \cdot MeOH$, $Cu_2(L_B)OH$, $Cu_2(L_A)Cl \cdot MeOH$, $Mn_2(L_A)OH \cdot 4H_2O$ and $Mn_2(L_B)OH \cdot H_2O \cdot MeOH$

The preparation was carried out by the same procedure used for the mononuclear nickel(II) complexes; Cu(OAc)$_2 \cdot 2H_2O$ (398 mg, 2 mmol), CuCl$_2 \cdot 2H_2O$ (341 mg, 2 mmol) and Mn(OAc)$_2 \cdot 6H_2O$ (490 mg, 2 mmol) were used instead of Ni(OAc)$_2 \cdot 6H_2O$. The deep green (for copper) and brown–yellow (for manganese) precipitates of the binuclear complexes were collected by filtration, washed with methanol/diethylether and dried *in vacuo*.

The same complexes can be prepared by using preformed ligands, instead of using template procedures.

$Na_2Cu_2(L_C)OH \cdot MeOH$, $Na_2Mn_2(L_C)OH \cdot 2MeOH$, $Na_2Ni_2(L_C)OH \cdot 3H_2O \cdot 2MeOH$, $Na_2Cu_2(L_D)OH \cdot 2H_2O \cdot 2MeOH$ and $Na_2Mn_2(L_D)OH \cdot H_2O \cdot MeOH$

To a methanolic solution of the ligand salt (Na$_5$-L$_C$ or Na$_5$L$_D$) (1 mmol), the appropriate metal salt (2 mmol), in water, was added. The solution became immediately deep green for copper or brown for

manganese derivatives. It was refluxed for 1 h, and then reduced in volume. After cooling, the precipitate obtained was filtered, washed with methanol, diethylether and dried *in vacuo*.

The same complexes have been obtained by using sodium salts of the ligands freshly prepared 'in situ'.

$Cu_2(H_2L_C)OH \cdot H_2O \cdot MeOH$

It was prepared by the same procedure used for the binuclear complexes derived from sulphonate ligands. (±)1-aminomethanephosphonic acid (2.51 mg, 2 mmol) was used instead of the corresponding aminosulphonic acid. A bright green product was obtained.

Elemental analysis for the prepared compounds is given in Table I.

X-ray Data

Crystals of $\{[Cu_2(C_{10}H_8ClN_2O_7S_2)(OH)](DMSO)\cdot(H_2O)\}_2$ suitable for the X-ray analysis were obtained by dissolving Cu$_2$(L$_A$)OH·MeOH in warm dimethyl-sulphoxide and maintaining the solution, after the addition of few drops of methanol, in an atmosphere saturated with diethylether.

Owing to the fact that the crystals decompose when isolated from the solution, a crystal fragment of maximum dimension 0.2 mm was introduced with the mother liquor into a glass capillary and well fixed and closed using another capillary of smaller dimension.

The X-ray work was performed on a Philips PW 1100 four-circle diffractometer using Mo Kα radiation. Cell parameters were obtained by least-squares refinement of 25 carefully determined angular settings. Crystal data: $\{[Cu_2(C_{10}H_8ClN_2O_7S_2)(OH)]\cdot(DMSO)(H_2O)\}_2$, formula weight 1215, orthorhombic, space group *Pbca*, general positions $\pm(x, y, z; \frac{1}{2}+x, \frac{1}{2}-y, z; x, \frac{1}{2}+y, \frac{1}{2}-z; \frac{1}{2}-x, y, \frac{1}{2}+z)$, with $a = 17.071(5)$, $b = 11.751(5)$, $c = 20.464(4)$ Å, $V = 4105$ Å^3, $D_c = 1.97$ g cm^{-3} for $Z = 4$ (there are four tetranuclear dimers in the unit cell which correspond to eight asymmetric units); μ(Mo Kα) = 12.9 cm^{-1}.

Intensities of 3620 reflexions were measured by the $\vartheta/2\vartheta$ scan method up to $2\vartheta = 50°$ with a scan rate of 2° min^{-1}. All data were corrected for Lorentz polarization and for absorption [8].

A total of 1723 intensities with $I > 3\sigma(I)$ were considered 'observed' and used in subsequent calculations.

The structure was solved by Patterson and Fourier methods and refined to the final *R* of 8.1% when the maximum shift on the refined parameters was 0.05σ. A final Fourier difference map showed no significant residuals.

Scattering factors for neutral atoms were taken from Cromer and Waber [9]. Ring carbon atoms were refined as rigid bodies (C–C = 1.395 Å);

TABLE I. Elemental Analysis for the Prepared Compounds

Compounds	Calculated (%)			Found (%)		
	C	H	N	C	H	N
$Na_3L_A \cdot 3H_2O$	24.46	2.85	5.70	24.75	2.60	5.67
$Na_3L_B \cdot 2H_2O \cdot MeOH$	29.29	3.76	5.25	29.09	3.73	5.18
$Na_5L_C \cdot 3H_2O \cdot 2MeOH$	26.83	4.18	4.47	26.76	4.09	4.48
$Na_5L_D \cdot 3H_2O$	25.62	3.22	4.98	25.94	3.34	4.65
$Cu_2(L_A)OH \cdot MeOH$	24.29	2.41	5.15	24.46	2.12	5.23
$Cu_2(L_A)Cl \cdot MeOH$	23.48	2.13	4.98	23.64	2.14	4.80
$Mn_2(L_A)OH \cdot 4H_2O$	21.19	3.02	4.94	20.92	3.11	4.66
$Cu_2(L_B)OH$	26.70	2.43	5.19	26.43	2.66	4.97
$Mn_2(L_B)OH \cdot H_2O \cdot MeOH$	27.26	3.34	4.89	27.35	3.48	4.59
$Cu_2(H_2L_C)OH \cdot H_2O \cdot MeOH$	26.47	3.59	4.77	26.73	2.93	4.77
$Na_2Ni_2(L_C)OH \cdot 3H_2O \cdot 2MeOH$	24.30	3.93	4.05	24.08	4.12	3.98
$Na_2Cu_2(L_C)OH \cdot H_2O \cdot MeOH$	24.64	3.02	4.42	24.51	2.91	4.22
$Na_2Mn_2(L_C)OH \cdot 2MeOH$	26.67	3.36	4.44	26.91	3.55	4.26
$Na_2Cu_2(L_D)OH \cdot 2H_2O \cdot 2MeOH$	24.59	3.69	4.10	24.00	2.83	3.88
$Na_2Mn_2(L_D)OH \cdot H_2O \cdot MeOH$	25.33	3.11	4.54	25.29	2.94	4.53
$Ni(L_E) \cdot 2H_2O$	29.11	2.99	3.77	29.24	2.94	3.76
$Ni(L_F) \cdot 2.5H_2O$	30.45	3.58	3.55	30.18	3.31	3.46

TABLE II. Atomic Parameters for $\{[Cu_2(L_A)(OH)](DMSO)(H_2O)\}_2$

Atom	x/a	y/b	z/c
Atomic coordinates			
Cu1	0.51588(13)	0.55707(18)	−0.06858(10)
Cu2	0.62887(13)	0.62498(19)	0.03260(11)
O1	0.55502(71)	0.69665(101)	−0.02739(59)
O3	0.58240(66)	0.48809(98)	−0.00026(56)
N1	0.65614(77)	0.77151(113)	0.06941(70)
N2	0.46668(85)	0.64457(129)	−0.14019(71)
Cl1	0.54782(37)	1.16927(44)	−0.11766(31)
S1	0.75553(30)	0.63676(47)	0.13074(23)
O11	0.70318(66)	0.55370(118)	0.09640(61)
O12	0.76954(93)	0.60246(149)	0.19700(81)
O13	0.82415(86)	0.66052(124)	0.09288(71)
S2	0.48096(32)	0.44425(48)	−0.19149(22)
O21	0.48893(82)	0.41699(108)	−0.11994(61)
O22	0.55616(80)	0.46757(116)	−0.22278(65)
O23	0.43269(79)	0.36071(119)	−0.22396(65)
O99	0.67842(99)	0.30687(144)	−0.01311(82)
C1	0.55556(68)	0.80329(70)	−0.04822(53)
C2	0.51245(68)	0.83224(70)	−0.10370(53)
C3	0.51083(68)	0.94480(70)	−0.12533(53)
C4	0.55230(68)	1.02840(70)	−0.09149(53)
C5	0.59540(68)	0.99944(70)	−0.03601(53)
C6	0.59703(68)	0.88689(70)	−0.01438(53)
C7	0.64347(108)	0.86563(177)	0.04631(91)
C8	0.69722(118)	0.76537(179)	0.13101(104)
C9	0.47135(97)	0.75071(152)	−0.14771(83)
C10	0.42393(106)	0.57561(160)	−0.18838(89)
S3	0.31666(31)	0.41205(49)	0.12431(26)
O31	0.27859(77)	0.35428(142)	0.06630(73)
C11	0.25780(186)	0.52635(265)	0.14706(123)
C12	0.29916(200)	0.32245(264)	0.19466(140)

TABLE II. *(continued)*

Atom	U_{11}	U_{22}	U_{33}	U_{23}	U_{13}	U_{12}
Thermal parameters[a] ($U_{ij} \times 10^{-4}$)						
Cu1	264(11)	232(11)	206(10)	3(11)	−29(10)	−19(11)
Cu2	250(11)	261(11)	309(12)	16(12)	−103(11)	−8(11)
O1	324(71)	251(66)	297(72)	−63(61)	−67(64)	−3(59)
O3	191(67)	206(63)	201(54)	8(52)	44(51)	−75(49)
N1	258(76)	200(75)	203(75)	53(71)	−140(71)	−65(60)
N2	287(89)	287(89)	280(84)	6(71)	−29(67)	61(70)
Cl1	700(41)	271(28)	630(38)	82(28)	−39(33)	3(28)
S1	299(25)	396(29)	302(25)	22(26)	−127(23)	4(23)
O11	168(62)	396(79)	399(75)	53(68)	−3(56)	73(62)
O12	644(49)					
O13	477(40)					
S2	366(28)	447(31)	212(23)	−82(25)	−28(22)	−29(27)
O21	535(89)	345(77)	280(68)	−48(61)	164(73)	17(71)
O22	410(36)					
O23	412(35)					
O99	648(49)					
C1	183(38)					
C2	284(43)					
C3	309(42)					
C4	333(47)					
C5	299(43)					
C6	270(42)					
C7	346(48)					
C8	391(50)					
C9	229(40)					
C10	297(44)					
S3	382(29)	511(34)	306(26)	−52(25)	40(25)	−69(26)
O31	350(80)	810(118)	446(85)	−249(95)	−64(71)	−189(80)
C11	942(215)	946(241)	561(165)	−474(170)	−274(164)	231(186)
C12	1273(275)	808(212)	562(175)	169(167)	27(185)	−258(209)

[a]Anisotropic thermal parameters are in the form: $T = \exp -2\pi^2 (U_{ij} H_i H_j A_i^* A_j^*)$.

hydrogen atoms were not introduced in the calculations. Calculations were performed using the SHELX program system [10]. Final atomic parameters are listed in Table II. Interatomic bond distances and angles are given in Tables III and IV. Table V reports the equations of mean planes through selected atomic groupings.

Physical Measurements

IR spectra were carried out as KBr pellets on a Perkin-Elmer 580B model Infrared Spectrophotometer. Electronic spectra at room temperature were carried out in dimethylsulphoxide for sulphonate derivatives, and as nujol mulls for phosphonate derivatives, on a Cary 17D model Spectrophotometer. Magnetic susceptibilities were determined by the Faraday method at room and at variable temperature ($Cu_2L_ACl \cdot MeOH$, $Cu_2L_AOH \cdot MeOH$, Cu_2L_BOH and $Na_2Cu_2L_DOH \cdot 2H_2O \cdot 2MeOH$) over the 67–300 K temperature region (Oxford Instruments) the apparatus being calibrated with $HgCo(NCS)_4$ [11]. Diamagnetic corrections were carried out [12].

TABLE III. Bond and Selected Contact Distances (Å)

Cu(1)–O(1)	1.96(1)	Cu(2)–O(1)	1.95(1)
Cu(1)–O(3)	1.98(1)	Cu(2)–O(3)	1.92(1)
Cu(1)–O(21)	2.01(1)	Cu(2)–O(11)	2.00(1)
Cu(1)–N(2)	1.98(1)	Cu(2)–N(1)	1.94(1)
S(2)–O(21)	1.50(1)	S(1)–O(11)	1.50(1)
S(2)–O(22)	1.46(1)	S(1)–O(12)	1.44(1)
S(2)–O(23)	1.44(1)	S(1)–O(13)	1.43(2)
S(2)–C(10)	1.83(2)	S(1)–C(8)	1.81(2)
N(2)–C(10)	1.47(2)	N(1)–C(8)	1.44(2)
N(2)–C(9)	1.26(2)	N(1)–C(7)	1.22(2)
C(2)–C(9)	1.49(2)	C(6)–C(7)	1.49(2)
C(1)–O(1)	1.32(1)	Cu(2)...O(31')	2.58(1)
S(3)–O(31)	1.51(1)	Cu(1)...Cu(2)	2.940(3)
S(3)–C(11)	1.74(3)	Cu(1)...Cu(1')	3.158(3)
S(3)–C(12)	1.81(3)	O(1)...O(3)	2.56(1)
Cl(1)–C(4)	1.742(9)	O(99)...O(3)	2.70(1)
		O(99)...O(31')	2.77(1)
		O(99)...O(13)	2.77(1)
		O(1)...O(3')	3.24(2)
		O(3)...O(3')	2.83(2)

' = 1 − x, 1 − y, 1 − z.

TABLE IV. Bond Angles (°)[a]

O(1)–Cu(1)–O(3)	81.0(5)	C(6)–C(7)–N(1)	124(2)
O(1)–Cu(1)–N(2)	91.6(6)	C(7)–N(1)–Cu(2)	128(1)
O(3)–Cu(1)–O(21)	99.5(5)	C(8)–N(1)–Cu(2)	114(1)
O(21)–Cu(1)–N(2)	86.6(6)	N(1)–C(8)–S(1)	108(1)
O(3)–Cu(1)–O(3')	83.6(5)	C(8)–S(1)–O(11)	102.6(9)
O(1)–Cu(2)–O(3)	82.8(5)	C(8)–S(1)–O(12)	109(1)
O(1)–Cu(2)–N(1)	90.9(5)	C(8)–S(1)–O(13)	106.8(9)
O(3)–Cu(2)–O(11)	98.0(5)	O(11)–S(1)–O(12)	111.1(9)
O(11)–Cu(2)–N(1)	88.1(6)	O(11)–S(1)–O(13)	111.2(8)
Cu(1)–O(1)–Cu(2)	97.4(5)	O(12)–S(1)–O(13)	115.5(9)
Cu(1)–O(3)–Cu(2)	98.2(5)	S(1)–O(11)–Cu(2)	114.3(8)
Cu(1)–O(3)–Cu(1')	96.4(5)	O(31)–S(3)–C(11)	108(1)
Cu(2)–O(3)–Cu(1')	106.6(5)	O(31)–S(3)–C(12)	107(1)
C(1)–O(1)–Cu(1)	131.0(9)	C(11)–S(3)–C(12)	98(2)
C(1)–O(1)–Cu(2)	127.4(9)	O(1)–Cu(1)–O(3')	100.5(5)
C(2)–C(9)–N(2)	126(1)		
C(9)–N(2)–Cu(1)	125(1)		
C(10)–N(2)–Cu(1)	115(1)		
N(2)–C(10)–S(2)	103(1)		
C(10)–S(2)–O(21)	101.2(8)		
C(10)–S(2)–O(22)	109.0(9)		
C(10)–S(2)–O(23)	106.7(8)		
O(21)–S(2)–O(22)	112.8(8)		
O(21)–S(2)–O(23)	110.8(8)		
O(22)–S(2)–O(23)	115.3(8)		
S(2)–O(21)–Cu(1)	110.8(7)		

[a]e.s.d.s. given in parentheses refer to the last significant digit.

TABLE V. Selected Planes, Lines and Distances (Å) of Atoms from the Planes[a]

Plane 1: O(1), O(3), O(11), N(1)
    $0.713X + 0.023Y - 0.700Z = 7.280$
    O(1), 0.06; O(3), −0.05; O(11), 0.05; N(1), −0.07;
    Cu(2), 0.081

Plane 2: O(1), O(3), O(21), N(2)
    $0.832X + 0.033Y - 0.553Z = 8.468$
    Cu(1), −0.145; the four atoms defining this plane are
    exactly coplanar

Plane 3: Cu(1), O(3), Cu(1'), O(3')
    $0.090X + 0.892Y + 0.444Z = 6.011$

Line 1: Cu(2), O(31)
$$-\frac{X - 7.746}{0.878} - \frac{Y - 5.754}{0.467} + \frac{Z - 1.012}{0.101}$$

Line 2: Cu(1), O(3')
$$-\frac{X - 7.968}{0.744} - \frac{Y - 6.281}{0.235} + \frac{Z + 0.699}{0.625}$$

Angles between planes and lines:

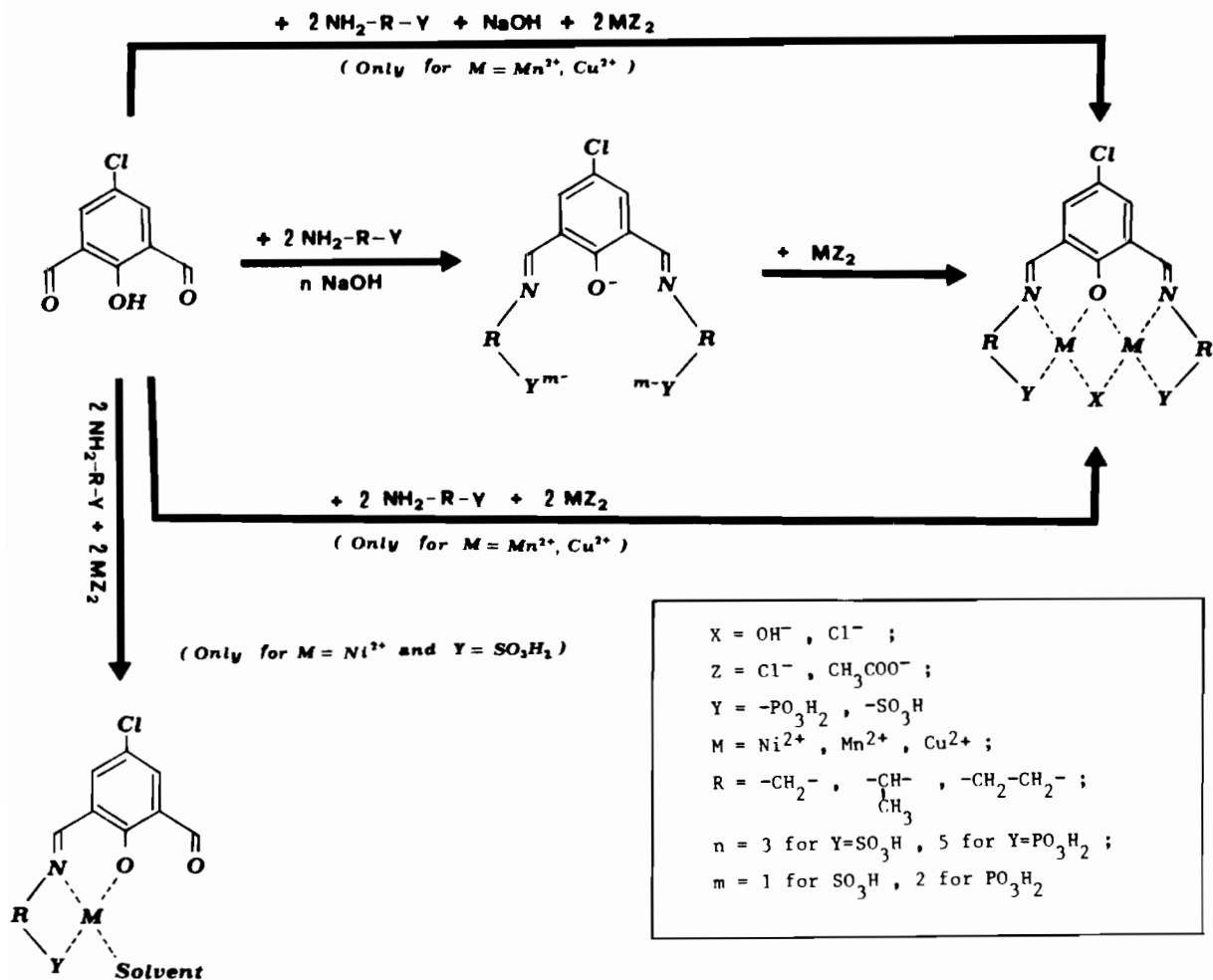| Planes	Angle (°)	Line–Plane	Angle (°)
1–2	10.9	1–1	45.1
1–3	76.9	2–2	76.7
2–3	81.9		

[a]X, Y and Z are orthogonal coordinates related to the fractional coordinates x, y and z by the matrix $X = 17.071x$; $Y = 11.751y$; $Z = 20.464z$.

Metal ratios were conveniently determined by the integral counting of back-scattered X-ray fluorescence radiation from a Philips SEM 505 model scanning electron microscope equipped with an EDAX model data station. Samples suitable for SEM analysis, were prepared by suspending the microcrystalline powders in petroleum ether 30–40°. Some drops of the resulting suspension were placed on a graphite plate and after evaporation of the solvent the samples were metallized with gold or graphite by using an Edward's S150 model sputter coater [13].

The electrochemical apparatus has been described elsewhere [14]. Potential values refer to an aqueous calomel electrode (S.C.E.). The temperature was controlled at 20 ± 0.1 °C. Under the present experimental conditions a potential value of +0.45 V is assigned to the ferrocene/ferrocenium couple in dimethylsulphoxide.

Results and Discussion

The ligands have been prepared as trisodium (for sulphonates) and pentasodium (for phosphonates) salts by reaction of 2,6-diformyl-4-chlorophenol with the appropriate amino acids (aminomethanesulphonic acid, 2-aminoethanesulphonic acid, (±)1-aminoethanephosphonic acid and 2-aminoethanephosphonic acid) in alcoholic solution and in the

Scheme 1.

Within the scheme box (right side):

$X = OH^-$, Cl^- ;

$Z = Cl^-$, CH_3COO^- ;

$Y = -PO_3H_2$, $-SO_3H$

$M = Ni^{2+}$, Mn^{2+} , Cu^{2+} ;

$R = -CH_2-$, $-\overset{|}{\underset{CH_3}{CH}}-$, $-CH_2-CH_2-$;

$n = 3$ for $Y=SO_3H$, 5 for $Y=PO_3H_2$;

$m = 1$ for SO_3H , 2 for PO_3H_2

presence of NaOH. The use of base is often necessary for these syntheses because the amino acids are in the zwitterionic form, as confirmed by the IR spectra.

Copper(II), nickel(II) and manganese(II) complexes have been synthesized following reaction procedures as in Scheme 1.

Binuclear complexes can be obtained by reaction of the preformed ligands with the appropriate metal acetate or chloride*. For copper(II) and manganese-(II) a template synthesis (without addition of NaOH) can be also used. Both procedures give the same sulphonate derivatives while the phosphonate complexes obtained by template synthesis contain two hydrogens instead of sodium.

In these complexes the exogenous bridge X is −OH or −Cl according to the type of metal salt used; the hydroxo group was found when metal acetate were employed.

Physico-chemical data suggest that nickel(II) gives, by the template procedure, the complexes $NiL_E \cdot 2H_2O$ and $NiL_F \cdot 2.5H_2O$ and by reaction with the preformed ligand $Na_5L_C \cdot 3H_2O \cdot 2CH_3OH$, the complex $Na_2Ni_2L_COH \cdot 3H_2O \cdot 2CH_3OH$.

By integration of back-scattered X-ray using a scanning electron microprobe, the metal, chlorine, sulphur (or phosphorous) and sodium, when present, ratios and the sample homogeneity were confirmed [13]. As an example Figs. 1 and 2 report the X-ray fluorescence spectra of the binuclear complexes of nickel(II) and manganese(II) with H_5L_C.

Na, P, Cl, Ni or Mn ratios are qualitatively 2:2:1:2. The quantitative electron microprobe analyses, which take in account autoabsorption phenomena (ZAF corrections), also give the same ratios inside the standard error.

The IR data (Table VI) show for the ligands broad bands in the range 1651−1522 cm⁻¹, for the bi-nuclear complexes sharp bands in the range 1647−1540 cm⁻¹; for nickel(II) mononuclear complexes a band at ≃1665 cm⁻¹ is attributable to $\nu(C=O)$

---

*It must be noted that the isomeric complexes derived from (±)1-aminoethanephosphonic acid have not been separated.
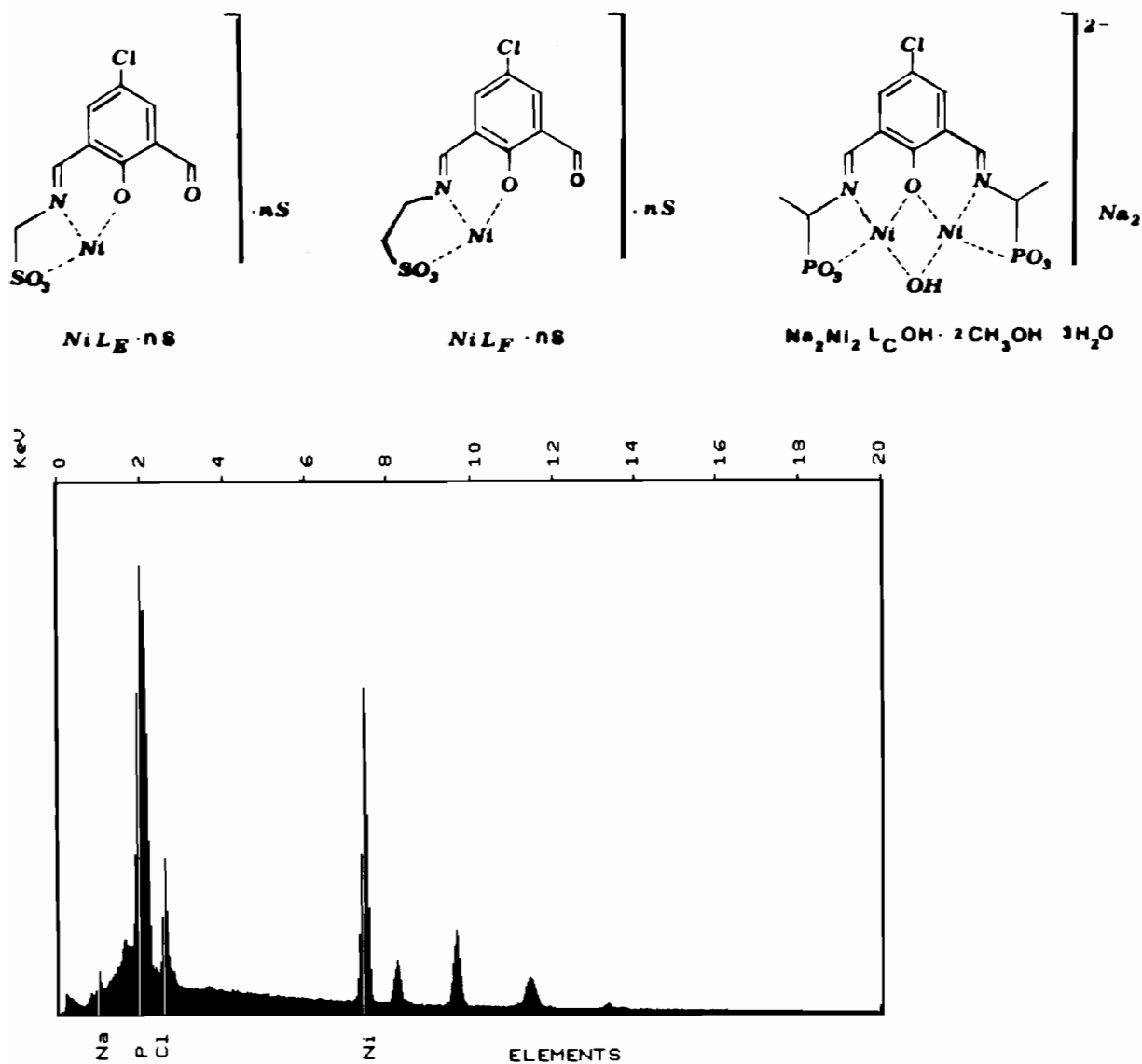
Fig. 1. X-ray fluorescence spectra of the binuclear complex $Na_2Ni_2L_COH\cdot3H_2O\cdot2MeOH$.

and a band at 1636 cm^{-1} to ν(C=N). Moreover there are absorptions in the range 1167–959 cm^{-1} attributable to PO_3^{2-} groups and in the range 1212–1037 cm^{-1} due to SO_3^- groups, respectively [15–17].

These bands, strong and broad, are diagnostic only of the presence of these groups and not of the coordination mode.

On going from the sodium salts of the ligands to the related complexes there is an increase in multiplicity of bands, associated for the phosphonate derivatives with a significant shift to higher frequencies.

The complexes $Cu_2(H_2L_C)OH\cdot H_2O\cdot MeOH$ and $Na_2Cu_2(L_C)OH\cdot H_2O\cdot MeOH$ have an almost identical

infrared spectrum also in the range of phosphonate absorptions.

The electronic spectra (Table VII) for copper(II) complexes show d–d bands in the range 720–750 nm in dimethylsulphoxide and at 740 nm in nujol mull which are in agreement, both in solution and in the solid, with a non-square planar structure. For manganese(II) complexes d–d bands in the range 890–900 nm have been found; nickel(II) complexes show bands or shoulders at 490, 485 and 435 nm.

Other bands or shoulders, in the range 330–250 nm in the electronic spectra of all the prepared complexes, are due to transitions within the ligands.
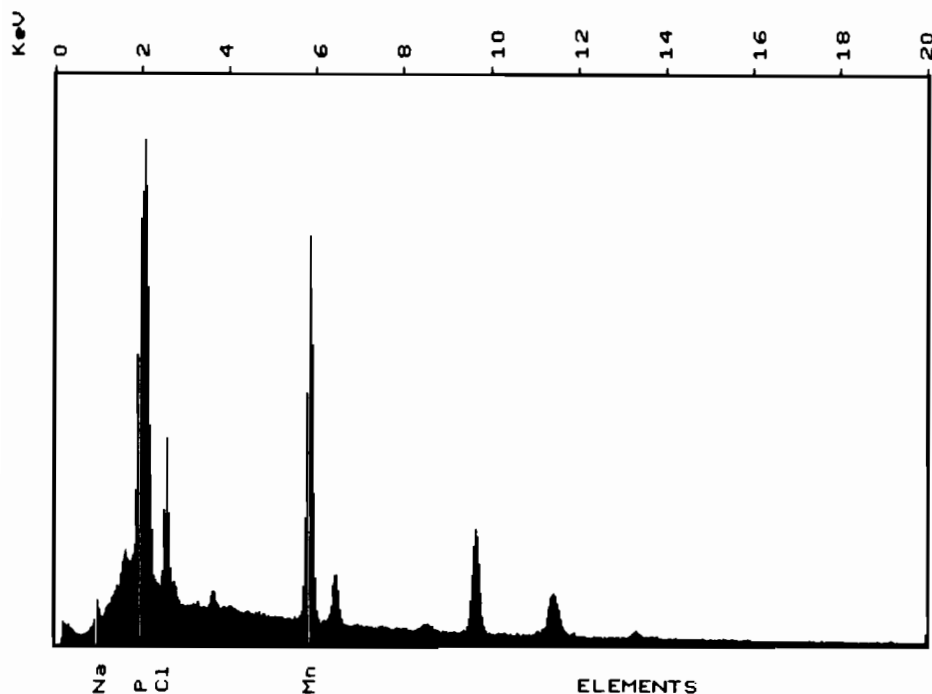
Fig. 2. X-ray fluorescence spectra of the binuclear complex $Na_2Mn_2L_COH \cdot 2MeOH$.

TABLE VI. Infrared Data (cm^{-1}) for the Prepared Compounds

Compounds	IR frequencies in the range 1700–1500 cm^{-1} assignable to $\nu(C=N)$, $\nu(C=O)$ and $\nu(C=C)$	Bands characteristic of $-SO_3^-$ and $-PO_3^{2-}$ groups
$Na_3L_A \cdot 3H_2O$	1646s, 1524s	1212b, 1051s
$Na_3L_B \cdot 2H_2O \cdot MeOH$	1651b, 1522s	1203b, 1054s
$Na_5L_C \cdot 3H_2O \cdot 2MeOH$	1646s, 1534s	1078b, 976s
$Na_5L_D \cdot 3H_2O$	1645s, 1526s	1068b, 984s
$Cu_2(L_A)OH \cdot MeOH$	1647s, 1561s	1192s, 1161b, 1077s
$Cu_2(L_A)Cl \cdot MeOH$	1647s, 1558s	1192s, 1162s, 1077s
$Mn_2(L_A)OH \cdot 4H_2O$	1647s, 1561s, 1542sh	1196s, 1166s, 1060s
$Cu_2(L_B)OH$	1646s, 1565s	1181s, 1156s, 1093s, 1036s
$Mn_2(L_B)OH \cdot H_2O \cdot MeOH$	1635s, 1540s	1186s, 1161s, 1047s
$Cu_2(H_2L_C)OH \cdot H_2O \cdot MeOH$	1645s, 1557s	1163s, 1114s, 1031s, 998s
$Na_2Ni_2(L_C)OH \cdot 3H_2O \cdot 2MeOH$	1652s, 1549s	1116s, 1054s, 964s
$Na_2Cu_2(L_C)OH \cdot H_2O \cdot MeOH$	1645s, 1559s	1132s, 1060s, 1028b, 959s
$Na_2Mn_2(L_C)OH \cdot 2MeOH$	1643s, 1543s	1115s, 1060s, 1037b, 972s
$Na_2Cu_2(L_D)OH \cdot 2H_2O \cdot 2MeOH$	1645s, 1565s	1155s, 1102s, 1051b, 970s
$Na_2Mn_2(L_D)OH \cdot H_2O \cdot MeOH$	1645s, 1545s	1167s, 1094s, 1063b, 989s
$Ni(L_E) \cdot 2H_2O$	1665s, 1636s, 1539s	1209s, 1160s, 1037s
$Ni(L_F) \cdot 2.5H_2O$	1660b, 1546s	1187s, 1162s, 1040s

Magnetic Measurements

The room temperature magnetic moments (Table VII) (μ_{eff}) for binuclear complexes are: $Cu_2(L_A)$-$OH \cdot CH_3OH$ (2.00 BM), $Cu_2(L_B)OH$ (2.17 BM), $Cu_2(L_A)Cl \cdot MeOH$ (1.88 BM), $Na_2Cu_2(L_D)OH \cdot 2H_2O$ $\cdot 2CH_3OH$ (2.49 BM), $Cu_2(H_2L_C)OH \cdot H_2O \cdot CH_3OH$ (2.50 BM) (the magnetic moment per copper atom is 1.33–1.77 BM, higher values for phosphonate analogues than sulphonate ones), $Mn_2(L_A)OH \cdot 4H_2O$ (7.19 BM), $Mn_2(L_B)OH \cdot H_2O \cdot CH_3OH$ (7.76 BM), $Na_2Mn_2(L_D)OH \cdot H_2O \cdot CH_3OH$ (7.70 BM), Na_2Mn_2-$(L_C)OH \cdot 2CH_3OH$ (7.64 BM) (the magnetic moment per manganese atom is 5.08–5.49 BM).

TABLE VII. Electronic (nm) and Magnetic (BM) Data for the Prepared Compounds

Compound	Electronic data (nm)	Magnetic moment (BM)
$Na_3L_A \cdot 3H_2O^a$	453s, 348s, 290sh	
$Na_3L_B \cdot 2H_2O \cdot MeOH^a$	460sh, 440s, 330sh, 270sh	
$Na_5L_C \cdot 3H_2O \cdot 2MeOH^b$	410s, 300sh, 260sh, 230sh	
$Na_5L_D \cdot 3H_2O^b$	455s, 325sh, 275sh, 250sh	
$Cu_2(L_A)OH \cdot MeOH^a$	720b, 425sh, 400s, 325sh	2.00
$Cu_2(L_A)Cl \cdot MeOH^a$	735b, 400s	1.88
$Mn_2(L_A)OH \cdot 4H_2O^a$	890b, 415s, 295sh	7.19
$Cu_2(L_B)OH^a$	750b, 387s	2.17
$Mn_2(L_B)OH \cdot H_2O \cdot MeOH^a$	900b, 410s, 300sh	7.76
$Cu_2(H_2L_C)OH \cdot H_2O \cdot MeOH$		2.50
$Na_2Ni_2(L_C)OH \cdot 3H_2O \cdot 2MeOH$		4.26
$Na_2Cu_2(L_C)OH \cdot H_2O \cdot MeOH^c$	740b, 440sh, 398s	
$Na_2Mn_2(L_C)OH \cdot 2MeOH$		7.64
$Na_2Cu_2(L_D)OH \cdot 2H_2O \cdot 2MeOH$		2.49
$Na_2Mn_2(L_D)OH \cdot H_2O \cdot MeOH^c$	445sh, 400s, 260s	7.70
$Ni(L_E) \cdot 2H_2O^a$	485sh, 435s, 315s, 300sh	2.97
$Ni(L_F) \cdot 2.5H_2O^a$	490w, 435s, 300sh, 265sh	3.03

[a]In dimethylsulphoxide.   [b]In methanol.   [c]As nujol mull.
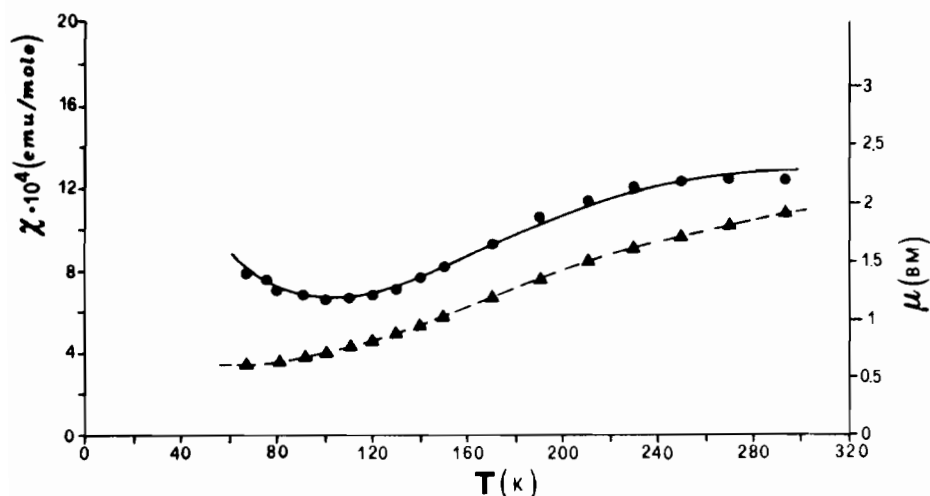
Fig. 3. Observed magnetic susceptibility (●) and effective magnetic moment (▲) *vs.* temperature for $Cu_2L_ACl \cdot MeOH$.

The magnetic moments for mononuclear nickel(II) complexes show the usual values for isolated nickel-(II) ions (μ_{eff} 2.97–3.03 BM). The binuclear complex $Na_2Ni_2(L_C)OH \cdot 3H_2O \cdot 2CH_3OH$ has a magnetic moment (μ_{eff}) of 4.26 BM (3.01 BM per nickel atom).

The observed (χ_{obs}) susceptibility and magnetic effective moments (μ_{eff})* of the complexes Cu_2L_A-Cl·MeOH, $Cu_2L_AOH \cdot MeOH$, Cu_2L_BOH and Na_2Cu_2-$L_DOH \cdot 2H_2O \cdot 2MeOH$ are reported in Figs. 3–6 (solid lines represent calculated susceptibilities) and Tables VIII–XI.

Magnetic parameters are derived from least-squares fitting by using the Bleaney–Bowers equation* [19, 20] corrected for the susceptibilities (χ_{param}) of possible paramagnetic impurity [21] and taking

---

*$\mu_{eff} = 2.828[(\chi_M - \chi_D)T]^{1/2}$ BM; $\chi_M = 2\chi_A$; χ_D represents the diamagnetic correction (see ref. 11).

---

*$\chi_M = \chi_{calc} = (1 - \rho)(6 \times 0.1251g^2)/[T(3 + e^{-2J/kT})] +$ TIP $+ \rho\chi_{param}$. The parameters reported in Table XII are obtained by minimizing the function $F = \Sigma_N(\chi_{obs} - \chi_{calc})^2$, where N is the number of measurements at different T. Although the structure of $Cu_2L_AOH \cdot MeOH$ could be tetrameric, on the basis of X-ray data for $\{[Cu_2L_AOH](DMSO)-(H_2O)\}_2$, the F/N value taken as a gauge of agreement between calculated and experimental values is small, when compared with actual experimental errors. Therefore, it has been possible to account for the magnetic properties of Cu_2L_A-OH·MeOH without any resort to 'tetramer' equation (see for instance ref. 18).
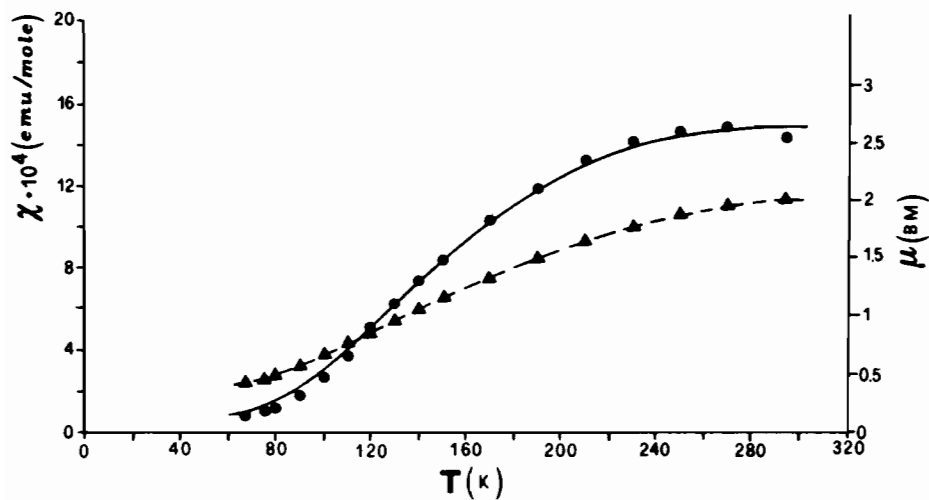
Fig. 4. Observed magnetic susceptibility (●) and effective magnetic moment (▲) *vs.* temperature for $Cu_2L_AOH \cdot MeOH$.
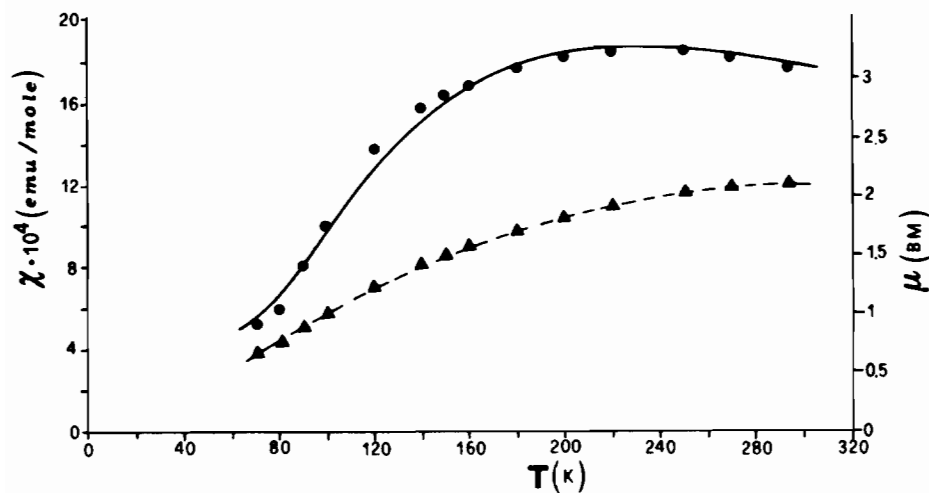

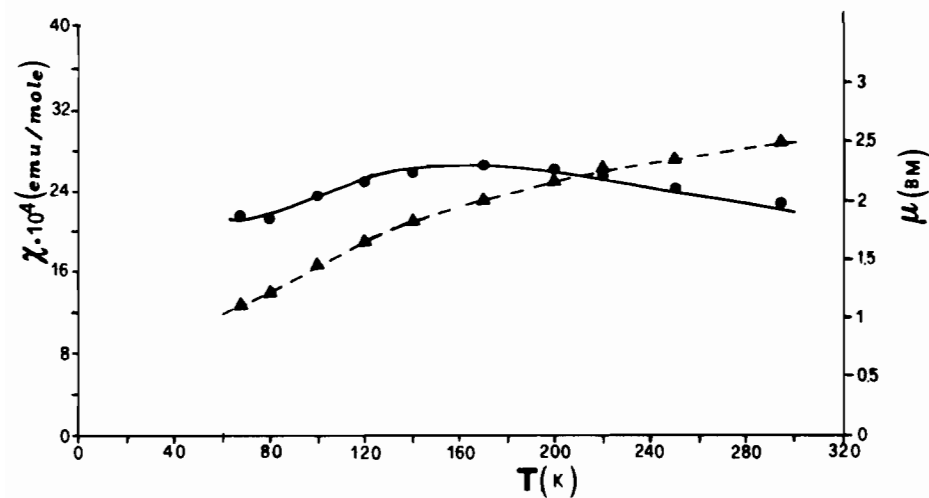Fig. 5. Observed magnetic susceptibility (●) and effective magnetic moment (▲) *vs.* temperature for Cu_2L_BOH.

Fig. 6. Observed magnetic susceptibility (●) and effective magnetic moment (▲) *vs.* temperature for $Na_2Cu_2L_DOH \cdot 2H_2O \cdot 2MeOH$.

TABLE VIII. Observed and Calculated Magnetic Susceptibility and Effective Magnetic Moment *versus* Temperature for $Cu_2L_ACl \cdot MeOH$ (see Fig. 3)

T	χ_{obs}	χ_{calc}	μ_{eff}
67	7.86	8.18	0.65
75	7.57	7.51	0.67
80	7.08	7.21	0.67
90	6.87	6.81	0.70
100	6.62	6.66	0.73
110	6.69	6.72	0.77
120	6.87	6.94	0.81
130	7.21	7.29	0.87
140	7.65	7.72	0.93
150	8.13	8.21	1.14
170	9.25	9.23	1.27
190	10.57	10.21	1.42
210	11.36	11.05	1.53
230	11.93	11.73	1.64
250	12.26	12.24	1.73
270	12.43	12.60	1.81
294	12.39	12.87	1.88

TABLE IX. Observed and Calculated Magnetic Susceptibility and Effective Magnetic Moment *versus* Temperature for $Cu_2L_AOH \cdot MeOH$ (see Fig. 4)

T	χ_{obs}	χ_{calc}	μ_{eff}
67	0.79	1.00	0.42
75	1.08	1.30	0.46
80	1.17	1.55	0.48
90	1.77	2.21	0.55
100	2.72	3.05	0.65
110	3.72	4.03	0.74
120	4.94	5.10	0.84
130	6.19	6.21	0.95
140	7.32	7.31	1.05
150	8.42	8.37	1.14
170	10.40	10.27	1.32
190	11.90	11.82	1.48
210	13.23	13.00	1.62
230	14.28	13.86	1.76
250	14.69	14.44	1.83
270	14.90	14.80	1.94
295	14.45	15.02	2.00

TABLE X. Observed and Calculated Magnetic Susceptibility and Effective Magnetic Moment *versus* Temperature for Cu_2L_BOH (see Fig. 5)

T	χ_{obs}	χ_{calc}	μ_{eff}
70	5.18	5.51	0.65
80	5.92	6.68	0.73
90	8.09	8.13	0.87
100	10.00	9.69	1.00
120	13.74	12.69	1.25
140	15.75	15.10	1.43
150	16.38	16.04	1.50
160	16.82	16.79	1.57
180	17.62	17.85	1.70
200	18.13	18.42	1.81
220	18.36	18.64	1.91
250	18.44	18.53	2.04
270	18.09	18.27	2.11
294	17.64	17.85	2.17

TABLE XI. Observed and Calculated Magnetic Susceptibility and Effective Magnetic Moment *versus* Temperature for $Na_2Cu_2L_DOH \cdot 2H_2O \cdot 2MeOH$ (see Fig. 6)

T	χ_{obs}	χ_{calc}	μ_{eff}
67	21.57	20.93	1.16
80	21.28	21.49	1.26
100	23.45	23.46	1.47
120	24.88	25.20	1.65
140	25.98	26.20	1.82
170	26.44	26.45	2.02
200	26.06	25.79	2.17
220	25.55	25.10	2.26
250	24.12	23.91	2.35
295	22.76	22.06	2.49

good crystals of Cu_2L_BOH for an X-ray diffraction analysis have failed so far. On the contrary, the $-J$ value for $Cu_2L_AOH \cdot MeOH$ is lower than that derived by applying the equation (see footnote on p. 112) to $Cu_2L_ACl \cdot MeOH$; however, some caution is needed in this case, since a remarkable amount of paramagnetic impurity is apparently present. The same is true when dealing with $Na_2Cu_2L_DOH \cdot 2H_2O \cdot 2MeOH$.

into account temperature-independent paramagnetism (TIP).

The g and J (antiferromagnetic) values observed in this series (Table XII) are in the usual range [22, 23] for complexes of analogous ligands and similar geometry (with reference, in particular, to the angles at the bridging atoms).

The absolute J value for $Cu_2L_AOH \cdot MeOH$ is significantly higher than for Cu_2L_BOH. This is certainly related to geometrical distortions introduced by a longer side chain. Attempts to obtain

X-ray Data
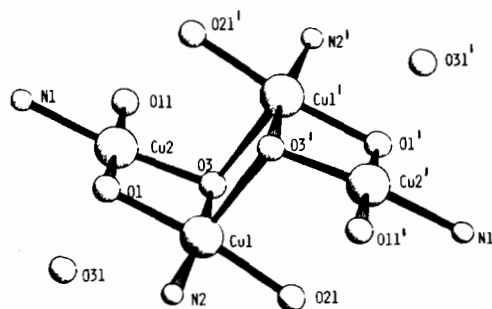
The crystal structure of the binuclear $Cu_2(L_A)OH$ complex, grown from dimethylsulphoxide solution, has been determined by X-ray crystallography. As shown in Fig. 7, the compound must be correctly formulated as $\{[Cu_2(L_A)(OH)](DMSO)(H_2O)\}_2$; the centrosymmetric molecule being formed by two binuclear units, one of which is the crystallographic asymmetric unit. The two binuclear units are parallel and form approximately planar moieties which are inclined by *ca.* 100° with respect to the set of four

TABLE XII. Magnetic Parameters of $Cu_2L_ACl \cdot MeOH$, $Cu_2L_AOH \cdot MeOH$, Cu_2L_BOH and $Na_2Cu_2L_DOH \cdot 2H_2O \cdot 2MeOH$

Compound	g	J	$T \times 10^4$	Paramagnetic impurity (%)	$(F/N) \times 10^8$
$Cu_2L_ACl \cdot MeOH$	2.09	200.9	0.90	6.0	0.04
$Cu_2L_AOH \cdot MeOH$	2.18	173.7	0.69		0.10
Cu_2L_BOH	2.06	129.6	1.09	1.8	0.19
$Na_2Cu_2L_DOH \cdot 2H_2O \cdot 2MeOH$	2.13	107.7	1.37	12.5	0.14
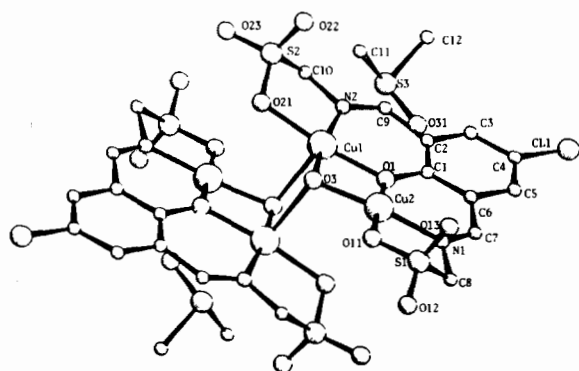
Fig. 7. The structure of $\{[Cu_2(L_A)(OH)](DMSO)(H_2O)\}_2$.

Fig. 8. Coordination around copper atoms in $\{[Cu_2(L_A)-$ $(OH)](DMSO)(H_2O)\}_2$.

transplanar atoms Cu(1), Cu(1′), O(3) and O(3′), so that the entire molecule adopts a chair configuration. Two independent copper ions, Cu(1) and Cu(2) are present in the asymmetric unit. Donor atoms for Cu(1), which is five-coordinated in the square pyramidal arrangement, are the phenato oxygen atom O(1), the hydroxo oxygen atom O(3), the sulphonato oxygen O(21), and N(2) as base atoms, the hydroxo oxygen atom O(3′) of the centrosymmetric unit being the axial atom. Donor atoms for Cu(2), which is square planar, are O(1), O(3), O(11) and N(2). As shown in Fig. 8, where the coordination geometries at the copper atoms are in evidence, Cu(2) also makes a contact of 2.58 Å with the oxygen atom O(31) of a DMSO molecule, which, in principle, could be considered a fifth donor atom. Nevertheless, there are three reasons to deem that this is not the case: (i) the actual distance is exceptionally long if compared with reported Cu–O (axial) distances in square pyramidal complexes; (ii) O(31) is strongly displaced from the apical position of the hypothetical square pyramidal arrangement (as shown in Table V the Cu(2)–O(31) line makes an angle of only 45° with the base plane) and there is no apparent ground for this; (iii) Cu(2) is only 0.08 Å out of the mean plane defined by the four donor atoms, which is within the limits of the deviations for slightly distorted square planar arrangements, while more significant displacements from the base plane are usually observed in square pyramidal coordination arrangements. On these bases Cu(2) can be considered

four-coordinate square planar, with an interaction with the DMSO molecule.

Cu–O (bridging) and Cu–N bond lengths (mean 1.95 and 1.96 Å respectively) compare well with values found in similar binuclear moieties, while Cu–O (sulphonato) distances are somewhat longer. The axial Cu(1)–O(3′) distance of 2.25 Å agrees with the value of 2.32 Å in $CuUO_2(aapen)(DMSO)_2$ [24], with 2.28 Å in $Cu_2(aapen) \cdot H_2O$ [25] (H_4aapen = 3,8-dimethyl-1,10-di(o-hydroxyphenyl)-4,7-diazadeca-2,8-diene-1,10-dione), with 2.31 Å in $\{Cu[2,5-bis(trifluoroacetyl)cyclopentanato](H_2O)\}_2$ [26], and with the axial Cu–N distance of 2.27 Å in [Cu(benzoylacetylacetonato)py]$_2$ [26]. It is noteworthy that the hydroxo oxygen atom O(3) is directly bridging three copper atoms, being coordinated to Cu(1) and Cu(2) in their base plane, and axially bonded to Cu(1), thus providing linkage of the two halves of the centrosymmetric molecule. Thus, the Cu(1)...Cu(2) separation of 2.94 Å between copper atoms of the same asymmetric unit is fully consistent with 2.96 Å found in $Cu_2(aapen)(H_2O)$, where the coordination geometries are the same as in the actual compound, while the Cu(1)...Cu(1′) separation between centrosymmetric atoms is longer (3.16 Å) because the bridging oxygen O(3) is involved in one basal and one (longer) axial bond with the corresponding copper atoms. No unusual features are present in the pentadentate ligand: C=N double bonds are well localized (mean value 1.24 Å), C–S bonds have the expected values (mean 1.82 Å), S–O (sulphonato) distances for the non-coordinated oxygen atoms are normal (mean 1.44 Å) and significantly shorter than corresponding distances (1.50 Å)
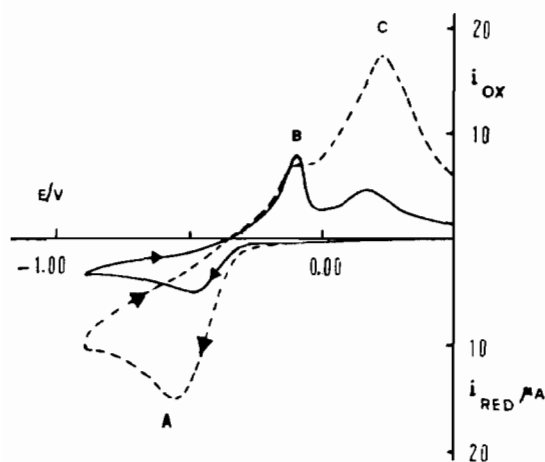
Fig. 9. Cyclic voltammograms recorded on a DMSO solution containing Cu_2L_BOH (1.04×10^{-3} mol dm^{-3}) and [NEt_4]-ClO_4 (0.1 mol dm^{-3}). ——, Scan rate 0.02 V s^{-1}. – – –, Scan rate 0.2 V s^{-1}. Platinum working electrode.

for the coordinated oxygens. The oxygen atoms of the two clathrate water molecules form relatively short contacts (2.70 to 2.77 Å) with O(3), O(13) and with the DMSO oxygen atom, which are within the range of commonly accepted hydrogen-bonded O...O separations.

Electrochemistry

The sulphonato complexes are soluble enough in dimethylsulphoxide to allow electrochemical studies; the low solubility of the phosphonato complexes in the organic solvents, precludes them from such an investigation. The complex Cu_2-(L_B)OH (Fig. 9) displays at a platinum electrode a single reduction peak A, to which the two peaks B and C are associated in the reverse scan. The scansion at the lowest rate of 0.02 V s^{-1} evidences the peak B to be due to the anodic stripping of copper metal electrodeposited on the indicator electrode.

Comparison with the response of an equimolar amount of the one-electron oxidizable ferrocene seems to indicate that the reduction process is in-

volving a one-electron charge transfer in the cyclic voltammetric time scale. On the contrary, 3 mol of electrons per mole of the complex were spent in the controlled potential coulometric tests at −0.9 V. This result does not agree either with the reduction to metal of one copper(II) centre, or with the reduction to metal of both copper(II) centres. The surprising circumstance that no copper metal was recovered on the working macroelectrode indicates that during the long period of electrolysis the electrogenerated copper metal is slowly sequestered by the ligand or its fragments. This aspect needs further investigation.

At mercury electrodes, strong adsorption phenomena prevented any reliable evaluation of the cathodic behaviour.

These data do not allow an unambiguous identification of the overall electrode process, with the exception of the short-time mechanism depicted in Scheme 2.
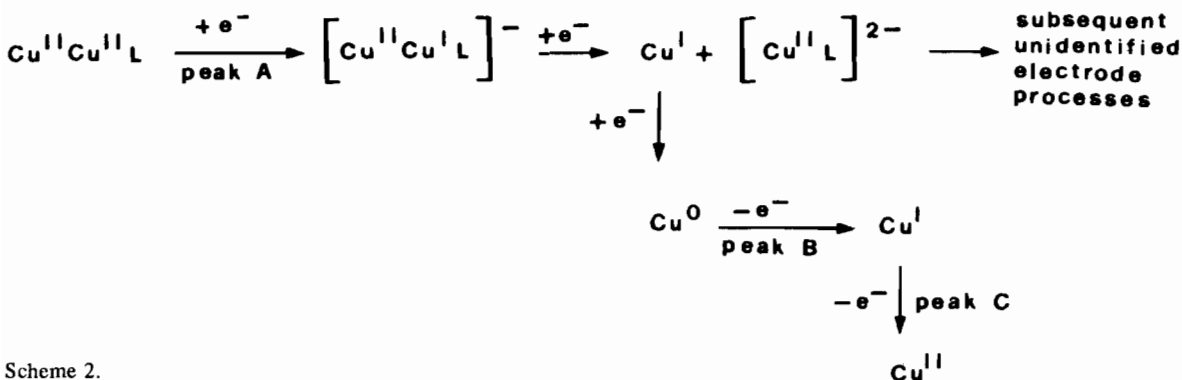
It was impossible to compete with the copper(I) decomplexation even using a scan rate of 50 V s^{-1}.

Both the less soluble hydroxo-bridged $Cu_2(L_A)\cdot$MeOH and the chloro-bridged $Cu_2(L_A)Cl\cdot MeOH$ display a qualitatively similar reduction pathway. Table XIII summarizes the potential values for the relevant $Cu^{II}Cu^{II}/Cu^{II}Cu^{I}$ charge transfers.

It is likely that the high rate of the decomplexation reaction of the electrogenerated $Cu^{II}Cu^{I}$ complex makes the reduction process appear electrochemically irreversible, so preventing the assignment of a thermodynamic potential to the relevant charge

TABLE XIII. Peak Potential Values (in volts *vs.* S.C.E.) for the One-electron Reduction of the Dicopper(II) Complexes in DMSO Solution

Complex	$Cu^{II}Cu^{II}/Cu^{II}Cu^{I}$
$Cu(L_A)OH\cdot MeOH$	−0.55
$Cu(L_B)OH$	−0.43
$Cu(L_A)Cl\cdot MeOH$	−0.43

$$Cu^{II}Cu^{II}L \xrightarrow[\text{peak A}]{+e^-} \left[Cu^{II}Cu^{I}L\right]^- \xrightarrow{+e^-} Cu^{I} + \left[Cu^{II}L\right]^{2-} \longrightarrow \begin{array}{l}\text{subsequent}\\\text{unidentified}\\\text{electrode}\\\text{processes}\end{array}$$

$$+e^- \downarrow$$

$$Cu^{0} \xrightarrow[\text{peak B}]{-e^-} Cu^{I}$$

$$-e^- \downarrow \text{peak C}$$

$$Cu^{II}$$

Scheme 2.

TABLE XIV. Redox Potentials (in volts *vs.* S.C.E.) for the Redox Changes of the Dimanganese(II) Complexes in DMSO Solution

Complex	$Mn^{II}Mn^{II}/Mn^{II}Mn^{I}$ [a]	$Mn^{II}Mn^{II}/Mn^{II}Mn^{III}$ [b]
$Mn_2(L_A)OH \cdot 4H_2O$	-0.95	$+0.70$
$Mn_2(L_B)OH \cdot H_2O \cdot MeOH$	-0.97	$+0.52$

[a]Computed as $1/2(E_{pc} + E_{pa})$. [b]Peak potential value at 0.2 V s^{-1}.
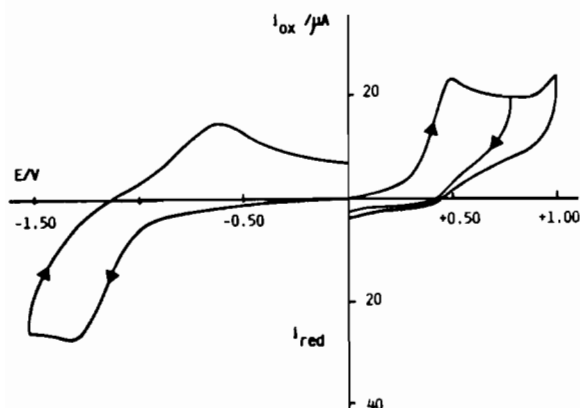
Fig. 10. Cyclic voltammetric behaviour at a platinum electrode of a DMSO solution containing $Mn_2(L_B)OH \cdot H_2O \cdot MeOH$ (1.5×10^{-3} mol dm^{-3}) and [NEt$_4$]ClO$_4$ (0.1 mol dm^{-3}). Scan rate 0.2 V s^{-1}.

transfer. It can only be argued that the cavity size in $Cu_2(L_B)OH$ would favour the tetrahedral rearrangement of the generated copper(I), so making easier its thermodynamic access, with respect to the situation of $Cu_2(L_A)OH \cdot MeOH$ and $Cu_2(L_A)Cl \cdot MeOH$.

Quite unexpectedly this does not actually seem to happen even if the non-thermodynamic significance of these redox potentials is considered. It is noteworthy that $Cu_2(L_B)OH$ and $Cu_2(L_A)Cl \cdot MeOH$ reduce at the same potential value, allowing us to think that the redox change is more governed by the geometry of the site than by the chemical nature of the bridging molecule. Uneasily rationalizable electrochemical responses are commonly given by hydroxo-bridged dicopper complexes [3].

The cyclic voltammetric behaviour at a platinum electrode of the dimanganese(II) complex $Mn_2(L_B)$-OH$\cdot$H$_2$O$\cdot$MeOH (Fig. 10), qualitatively constant in the scan rate range from 0.02 to 50 V s^{-1}, evidences both a cathodic process, at the boundaries of the electrochemical quasi-reversibility, and an irreversible anodic process. By comparison with the response from ferrocene, both the processes involve a one-electron charge transfer in the time scale of cyclic voltammetry, and can be attributed to the $Mn^{II}Mn^{II}/Mn^{II}Mn^{I}$ and $Mn^{II}Mn^{II}/Mn^{II}Mn^{III}$ charge transfers, respectively.

Also in this case severe electrode poisonings occur at mercury electrodes.

The same behaviour was observed for the dimanganese(II) complex $Mn_2(L_A)OH \cdot 4H_2O$ (Table XIV).

On the basis of the above results the compartmental behaviour of the prepared ligands is proved. The different behaviour with respect to the ligands derived from 2-amino-5-methyl-benzenesulphonic or 2-aminonaphthalenesulphonic acids, is due to their pronounced flexibility.

Acknowledgements

References

1 U. Casellato, P. A. Vigato and M. Vidali, *Coord. Chem. Rev., 23*, 31 (1977).
2 U. Casellato, P. A. Vigato, D. E. Fenton and M. Vidali, *Chem. Soc. Rev., 8*, 199 (1979).
3 P. Zanello, S. Tamburini, P. A. Vigato and G. A. Mazzocchin, *Coord. Chem. Rev., 77*, 165 (1987).
4 D. E. Fenton, in A. G. Sykes (ed.), 'Advances in Inorganic and Bioinorganic Mechanisms', Vol. 2, Academic Press, London, 1983, p. 187.
5 J. M. Bellerby, J. H. Morris and W. E. Smith, *Inorg. Chim. Acta, 102*, 121 (1985), and refs. therein.
6 P. Guerriero, D. Ajò', P. A. Vigato, U. Casellato and S. Tamburini, *Inorg. Chim. Acta, 120*, L9 (1986).
7 A. Zinke, F. Hanus and E. Ziegler, *J. Prakt. Chem., 152*, 126 (1939).
8 A. C. T. North, D. C. Phillips and F. S. Mathews, *Acta Crystallogr., Sect. A, 24*, 351 (1968).
9 D. T. Cromer and J. T. Waber, *Acta Crystallogr., 18*, 104 (1965).
10 G. M. Sheldrick, 'SHELX', program for crystal structure determination, University of Cambridge, U.K., 1975.
11 H. St Rade, *J. Chem. Phys., 77*, 424 (1973).
12 Ch. J. O'Connor, in S. J. Lippard (ed.), 'Progress in Inorganic Chemistry', Vol. 29, Wiley, New York, 1982, pp. 208–211.
13 U. Casellato, P. Guerriero, S. Tamburini, P. A. Vigato and R. Graziani, *Inorg. Chim. Acta, 119*, 215 (1986).
14 D. Osella, R. Gobetto, P. Montangero, P. Zanello and A. Cinquantini, *Organometallics, 5*, 1247 (1986).

15 L. J. Bellamy, 'The Infrared Spectra of Complex Molecules', Wiley, New York, 1986.
16 N. B. Colthup, L. H. Daly and S. E. Wiberley, 'Introduction to Infrared and Raman Spectroscopy', Academic Press, London, 1975.
17 J. M. Bellerby, J. H. Morris and W. E. Smith, *Inorg. Chim. Acta, 96*, 203 (1985).
18 W. E. Hatfield and G. W. Inman, Jr., *Inorg. Chem., 8*, 1376 (1969).
19 E. E. Eduok and Ch. J. O'Connor, *Inorg. Chim. Acta, 88*, 229 (1984).
20 A. Earnshaw, 'Introduction to Magnetochemistry', Academic Press, London, 1968.

21 O. Kahn, I. Morgenstern-Badarau, J. P. Audiere, J. M. Lehn and S. A. Sullivan, *J. Am. Chem. Soc., 102*, 5935 (1980), and refs. therein.
22 V. H. Crawford, H. W. Richardson, J. R. Wasson and D. J. Hodgson, *Inorg. Chem., 15*, 2107 (1976).
23 D. J. Hodgson, in S. J. Lippard (ed.), 'Progress in Inorganic Chemistry', Vol. 19, Wiley, New York, 1980.
24 R. Graziani, M. Vidali, U. Casellato and P. A. Vigato, *Transition Met. Chem., 3*, 239 (1978).
25 R. Graziani, M. Vidali, U. Casellato and P. A. Vigato, *Transition Met. Chem., 3*, 138 (1978).
26 R. L. Lindvedt, M. D. Glick, B. K. Tomlonovic, D. P. Gavel and J. M. Kuszaj, *Inorg. Chem., 15*, 1633 (1976).